Supporting Information

A first-principles-based sub-lattice formalism for predicting off-stoichiometry in materials for solar thermochemical applications: the example of ceria

*Gopalakrishnan Sai Gautam, Ellen B. Stechel and Emily A. Carter**

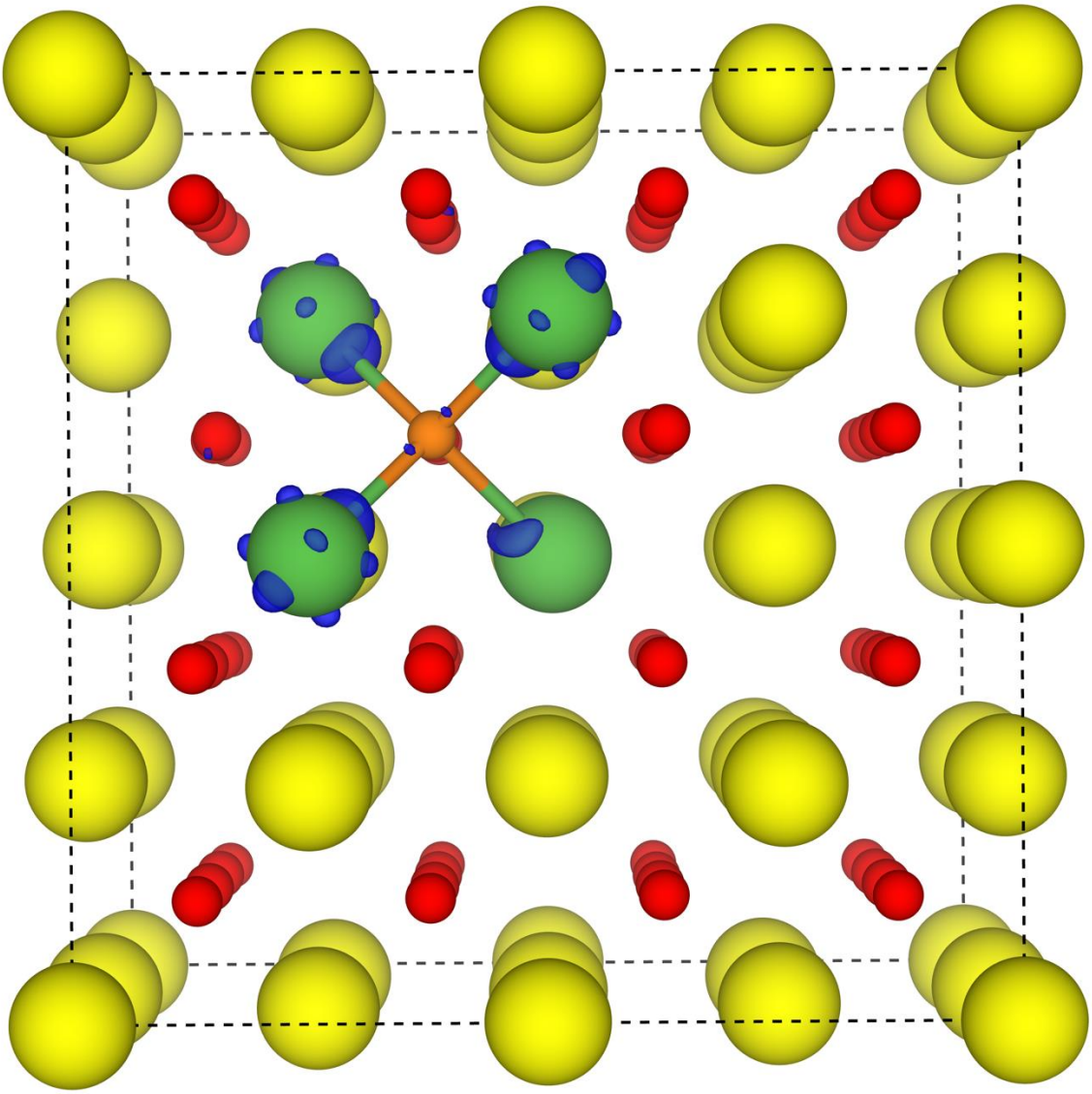

Figure S1. Difference in electron density between pure and defective CeO_2. Yellow and red spheres respectively correspond to Ce and O ions, while the orange and green spheres respectively signify the oxygen vacancy (Va_O) and Ce ions that are nearest neighbors (NN) to the Va_O. Blue isosurfaces indicate regions of electron accumulation when a Va_O is created, with the isosurface set to 0.009 e/bohr^3. Thus, the electrons generated due to a Va_O tend to reduce the NN Ce atoms, with some delocalization amongst the NN Ce, as highlighted by the presence of blue isosurfaces on all four NN Ce.

S1 Errors due to excluding temperature dependence when estimating the oxygen chemical potential

The mathematical expression for the oxygen chemical potential (μ_{O}) in $\mathrm{CeO}_{2-\delta}$ can be derived by differentiating $G^{\mathrm{F}}_{\mathrm{CeO_x}}$ in **Equation 23** in the main text with respect to $\delta = 2 - x$, and can be written as follows.

$$\mu_{\mathrm{O}} = -\frac{dG^{\mathrm{F}}_{\mathrm{CeO}_{2-\delta}}}{d\delta} = 2\left[G^{\mathrm{F}}_{\mathrm{CeO}_2} - G^{\mathrm{F}}_{\mathrm{CeO}_{1.5}}\right] + 4RT\left\{\frac{3}{4}\ln\frac{3}{4} + \frac{1}{4}\ln\frac{1}{4}\right\} + (8\delta - 2)(L_0 - L_1) + (48\delta^2 - 16\delta)L_1 - RT\left[2\ln\left(\frac{2\delta}{1-2\delta}\right) + \ln\left(\frac{\delta}{2-\delta}\right)\right] \quad \text{(S1)}$$

Thus, μ_{O} in **Equation S1** can be split into three-components, namely, $\mu_{\mathrm{O}}^{\mathrm{end-members}}$, $\mu_{\mathrm{O}}^{\mathrm{excess}}$, μ_{O}^{S}, which arise from $G^{\mathrm{end-members}}$, G^{excess}, and S^{soln}, respectively. Specifically, the expressions for the three μ_{O} components are,

$$\mu_{\mathrm{O}}^{\mathrm{end-members}} = 2\left[G^{\mathrm{F}}_{\mathrm{CeO}_2} - G^{\mathrm{F}}_{\mathrm{CeO}_{1.5}}\right] + 4RT\left\{\frac{3}{4}\ln\frac{3}{4} + \frac{1}{4}\ln\frac{1}{4}\right\}$$

$$\mu_{\mathrm{O}}^{\mathrm{excess}} = (8\delta - 2)(L_0 - L_1) + (48\delta^2 - 16\delta)L_1$$

$$\mu_{\mathrm{O}}^{S} = -RT\left[2\ln\left(\frac{2\delta}{1-2\delta}\right) + \ln\left(\frac{\delta}{2-\delta}\right)\right] \quad \text{(S2)}$$

While the μ_{O}^{S} employed in this work is identical to the model of Zinkevich et al.,[67] we do not account for the temperature dependence of $G^{\mathrm{F}}_{\mathrm{CeO}_2}$ and $G^{\mathrm{F}}_{\mathrm{CeO}_{1.5}}$ in $\mu_{\mathrm{O}}^{\mathrm{end-members}}$ and L_0 and L_1 in $\mu_{\mathrm{O}}^{\mathrm{excess}}$, which can contribute to discrepancies between the two models. To better quantify the sensitivity of the temperature-dependent contributions, we plot variation in μ_{O} with temperature (from 300-1700 K) in **Figure S2**, with and without the temperature dependence of the end-member and excess terms. Specifically, we plot two distinct scenarios where we include only $\mu_{\mathrm{O}}^{\mathrm{end-members}}$ (panel a in Figure S2), and $\mu_{\mathrm{O}}^{\mathrm{end-members}} + \mu_{\mathrm{O}}^{\mathrm{excess}}$ (panel b). Since $\mu_{\mathrm{O}}^{\mathrm{excess}}$ is dependent on δ, we set $\delta \to 0$ in Figure S2b. Additionally, the absolute values of all μ_{O} components are calculated using the

values provided by Zinkevich et al.[67] to accurately quantify the errors due to excluding the temperature-dependence.

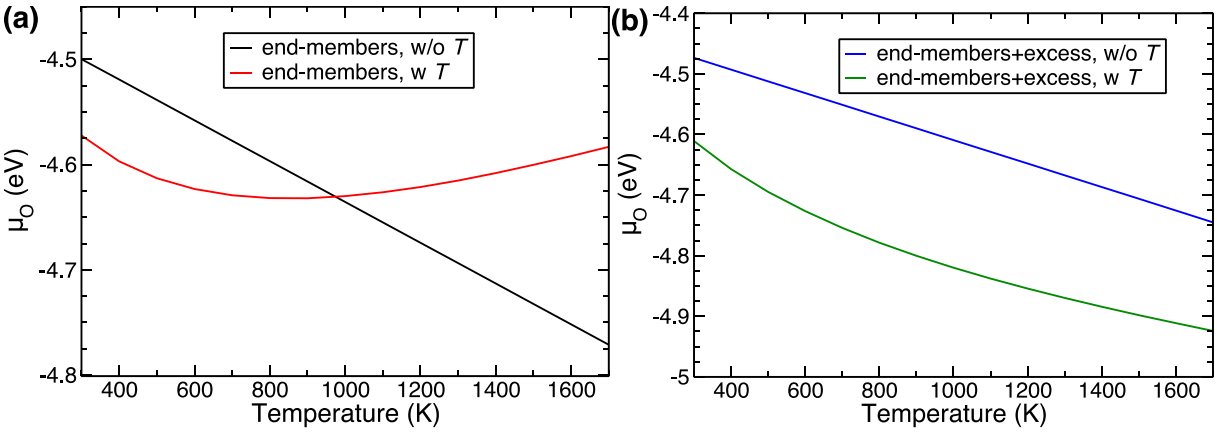

Figure S2. Variation of the oxygen chemical potential in $CeO_{2-\delta}$ with temperature is plotted including only the end-member contributions (panel a), and end-member+excess components (panel b). The legends "w *T*" and "w/o *T*" indicate including and excluding the temperature-dependences of the end-member and excess terms.

Although $\mu_O^{end-members}$ (in Figure S2a) displays qualitative differences between excluding ("w/o *T*", black line), and including ("w *T*", red curve) temperature dependence, the absolute differences between the two scenarios is quite low. For example, the maximum deviation w and w/o *T* in $\mu_O^{end-members}$ is ~4% (at 1700 K). However, adding the μ_O^{excess} component (panel b) reduces the qualitative differences between w/o *T* and w *T* scenarios (both μ_O decrease monotonically with temperature), with the magnitude of deviation ranging from 3% to 4.6%, signifying a similar magnitude of error across all temperatures.